Agricultural and Forest Meteorology 149 (2009) 1118–1128

Contents lists available at ScienceDirect

Agricultural and Forest Meteorology

journal homepage: www.elsevier.com/locate/agrformet

Long-term climate change impacts on agricultural productivity in eastern China

Daniel R. Chavas [a,*], R. César Izaurralde [a], Allison M. Thomson [a], Xuejie Gao [b]

[a] Joint Global Change Research Institute, Pacific Northwest National Laboratory and the University of Maryland, College Park, 8400 Baltimore Ave. Suite 201, College Park, MD 20740, USA
[b] National Climate Center, China Meteorological Administration, Beijing, China

ARTICLE INFO

Article history:
Received 16 July 2008
Received in revised form 26 January 2009
Accepted 2 February 2009

Keywords:
China
Crop productivity
EPIC model
Impacts
Global warming

ABSTRACT

Increasing atmospheric greenhouse gas concentrations are expected to induce significant climate change over the next century and beyond, but the impacts on society remain highly uncertain. This work examines potential climate change impacts on the productivity of five major crops in eastern China: canola, corn, potato, rice, and winter wheat. In addition to determining domain-wide trends, the objective is to identify vulnerable and emergent regions under future climate conditions, defined as having a greater than 10% decrease and increase in productivity, respectively. Data from the ICTP RegCM3 regional climate model for baseline (1961–1990) and future (2071–2100) periods under A2 scenario conditions are used as input for the EPIC agro-ecosystem simulation model in the domain [30°N, 108°E] to [42°N, 123°E]. Simulations are performed with and without the enhanced CO_2-fertilization effect. Results indicate that aggregate potential productivity (i.e. if the crop is grown everywhere) increases 6.5% for rice, 8.3% for canola, 18.6% for corn, 22.9% for potato, and 24.9% for winter wheat, although with significant spatial variability for each crop. However, without the enhanced CO_2-fertilization effect, potential productivity declines in all cases ranging from 2.5 to 12%. Interannual yield variability remains constant or declines in all cases except rice. Climate variables are found to be more significant drivers of simulated yield changes than changes in soil properties, except in the case of potato production in the northwest where the effects of wind erosion are more significant. Overall, in the future period corn and winter wheat benefit significantly in the North China Plain, rice remains dominant in the southeast and emerges in the northeast, potato and corn yields become viable in the northwest, and potato yields suffer in the southwest with no other crop emerging as a clear beneficiary from among those simulated in this study.

1. Introduction

Climate change has gained significant international attention over the past decade due to concerns of deleterious long-term impacts on agriculture, water supply, human welfare, and regional political stability. According to the IPCC Fourth Assessment Report (IPCC, 2007), global mean temperatures have risen approximately 0.74 °C in the last 100 years. The majority of this warming has occurred since 1950 and is very likely due to anthropogenic activities that have elevated greenhouse gas concentrations to unprecedented levels in recent history. Global climate models (GCMs) predict temperature increases of 1.1–6.4 °C over the period 1990–2100. However, the resulting impacts are highly dependent on regional variability (Tan and Shibasaki, 2003), the uncertainty of which constrains our capacity to determine optimal responses for adaptation.

In the case of agriculture, changes in temperature, precipitation, wind speed, and atmospheric CO_2 concentration can all have significant impacts on crop productivity, rendering it perhaps the most sensitive to climate change among all key economic sectors (Downing, 1996; Watson et al., 1996). This is of particular importance in China, comprising 22% of the global population and only 7% of the global supply of arable land (Tong et al., 2003), which is undergoing a period of rapid economic development that has persisted over the past 30 years (US DOE, 2004). Furthermore, approximately 30% of total food production in China comes from rain-fed agriculture, much of which is located in the drought-prone northeast (Tao et al., 2003; Qian and Zhu, 2001). For example, the Huang-Hai Plain (HHP), known as the "bread basket" of China (World Bank, 2002), has only 7.7% of national water resources, yet it produces 39.2% of national grain supply and 32.4% of gross domestic product (Tian, 2006). Thus, the ability to meet future demand may hinge on proper assessment of medium- and long-term agricultural vulnerability to climate change and the measures taken to adapt accordingly (Lin, 1996).

* Corresponding author. Tel.: +1 773 936 4510.
E-mail address: drchavas@mit.edu (D.R. Chavas).

0168-1923/$ – see front matter © 2009 Elsevier B.V. All rights reserved.
doi:10.1016/j.agrformet.2009.02.001

Prior studies have examined potential climate change impacts on agriculture in this region. In the Huang-Hai Plain, GCM projections of decreased precipitation, as well as socioeconomic circumstances, would render winter wheat (*Triticum aestivum* L.) and corn (*Zea mays* L.) production more vulnerable to climate change (Lin, 1996). Tao et al. (2003) found variable results for impacts on winter wheat and corn productivity in the region due to soil moisture deficits. Thomson et al. (2006) examined the role of tillage in climate change impacts on agricultural productivity and soil carbon sequestration. At the national scale, Lin et al. (2005) used the PRECIS regional climate model and the CERES crop model to analyze impacts of climate change and CO_2 fertilization on crop productivity for both the A2 and B2 SRES scenarios and found highly variable results for wheat, corn, and rice (*Oryza sativa* L.) depending on scenario and irrigation practice. Xiong et al. (2007) extended this approach to examine impacts on maize in greater detail and found yield increases for rain-fed corn but decreases for irrigated corn with the CO_2 enrichment included. Tao et al. (2008) found largely negative climate change impacts on rice production in China using a probabilistic approach.

This work seeks to contribute to the global climate change impacts assessment effort by using a simulation modeling approach to assess the long-term regional-scale changes in agricultural productivity in eastern China under a future climate scenario in which minimal reductions in greenhouse gas emissions have occurred, based upon output from a high-resolution regional climate model. Five crops were selected for analysis based upon their relative abundance in the region's agricultural output: canola (*Brassica napus* L.), corn, potato (*Solanum tuberosum* L.), rice, and winter wheat. Each crop is simulated on all agricultural land within the domain under baseline and future climate conditions in order to assess the relative changes in potential productivity due to climate change under traditional management practices. The primary goal is to gain insight into potential regions of significant increase ("emergent regions") or decrease ("vulnerable regions") for adaptation purposes.

2. Methods

The general approach of this study is to examine climate change impacts on agricultural productivity in eastern China by combining regional climate model output (RegCM3) over the domain, a global soil database (WISE), a county-level cropland database (UNH), and Chinese farm management data with the EPIC agro-ecosystem simulation model. Descriptions of the datasets are provided below. Comparison of EPIC model output for baseline (1961–1990) and future (2071–2100) periods provide insight into how crop yields may change under the IPCC SRES A2 climate scenario (described below).

2.1. Study region characteristics

The domain of interest extends from [30°N, 108°E] to [42°N, 123°E] (Fig. 1) and is a key region of agricultural and economic activity. It includes most or all of the provinces and municipalities of Hebei, Beijing, Tianjin, Shanxi, Shandong, Shaanxi, Henan, Jiangsu, Hubei, Anhui, and Shanghai. The climate in the south-eastern third of the domain is characterized as warm humid, the northwestern third as cold semi-arid, and the intermediate strip as warm sub-humid (Soil Map of the People's Republic of China, 1990). Overall, the climate is dominated by the East Asian Monsoon with greater influence from mid-latitude weather systems to the north (Tao and Chen, 1987; Cheng, 1993), with a predominant northwest to southeast gradient in mean temperature and total annual precipitation and a distinct May–September rainy season.

Dominant soil zones in the region are closely linked to the spatial distribution of climatic and geomorphologic features (Canpeng et al., 1999). Fluvisols are the predominant soil type, with Lithosols, Cambisols, and Gleysols also present in the region (Soil Map of the People's Republic of China, 1990).

Fig. 2 displays a map of the dominant crop by county. Rice is primarily grown in the southeast and secondarily in the northeast; potato is grown primarily in the southwest; winter wheat and cotton are grown primarily in the center of the domain; corn, canola, potato, and sorghum are grown in the north.

2.2. Climate scenario

The climate change projections are taken from the ICTP RegCM3 regional climate model simulations (Gao et al., 2008) for the baseline period 1961–1990 and the future period 2071–2100 under IPCC SRES A2 scenario conditions. This model is nested within the NASA/NCAR global FvGCM to downscale results from this large-scale GCM to a high resolution of 20 km grid spacing over China, from which a .25 × .25 degree grid is created for this study. The higher resolution enables much improved representation of topography and the key climatic features (e.g. the monsoon) that it modulates (Gao et al., 2008). Monthly climate statistics for the two periods are shown in Table 1. Daily weather files taken directly from RegCM3 output are used as input necessary to drive the Environmental Policy Integrated Climate (EPIC) model (Williams, 1995).

The A2 scenario describes a very heterogeneous world of high population growth, slow economic development and strong regional cultural identities, and thus has significant climate change due to substantially higher rates of atmospheric CO_2 accumulation (Nakicenovic et al., 2000). Concentrations of CO_2 approach 850 ppmv by 2100.

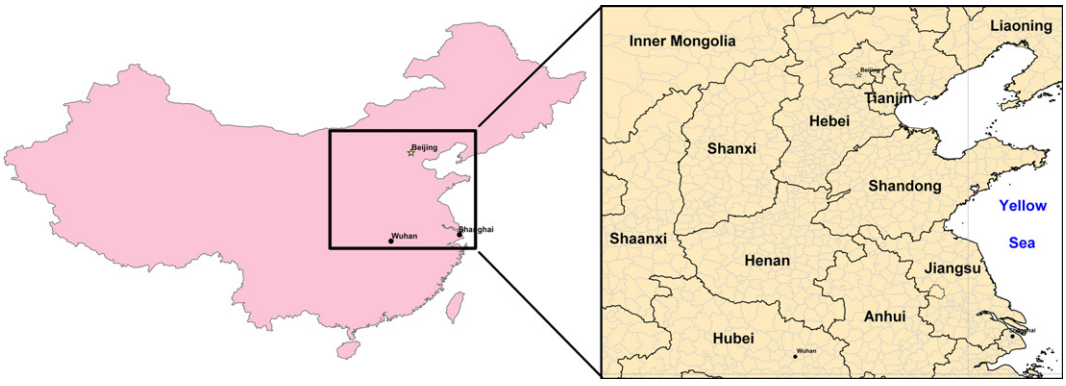

Fig. 1. Map of domain of interest extending from [30°N, 108°E] to [42°N, 123°E].

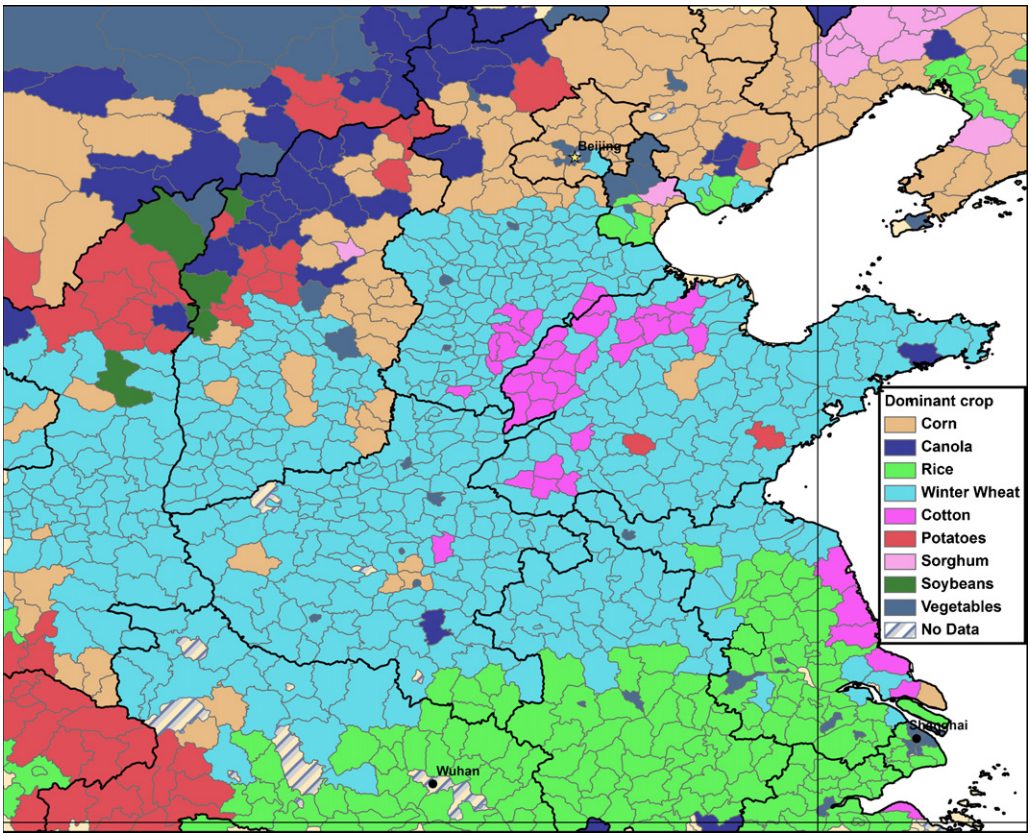

Fig. 2. Dominant crop by county, based on 1990 UNH county-level cropland database (Li et al., 2003).

2.3. Soil database

The soil properties used in this study are taken from the International Soil Reference and Information Centre (ISRIC) World Inventory of Soil Emission Potentials (WISE) soil polygon dataset (Batjes, 2006) with 5 by 5 arc-minute resolution on a global grid. The WISE database disaggregates each soil polygon into a set of soil profiles and their proportional areal coverage within that polygon. Each soil profile is composed of five layers, each with a depth of 20 cm, and contains data for 19 soil variables that are commonly required for agro-ecological studies. Data on layer depth (LayerD), bulk density (BD), soil texture, pH, soil carbon content, calcium carbonate content, and cation exchange capacity are used to initialize the EPIC model run at each location.

2.4. Cropland database

Data of cropland area for each of 48 single and multiple crop rotations in each county is taken from the 1990 county-level database used in Li et al. (2003) and maintained by the University of New Hampshire EOS-WEBSTER Earth Science Information Partner (ESIP) (http://eos-webster.sr.unh.edu/home.jsp; *Ecological Archives* A013-006-A1). The database is derived from a combination of a county statistical database on

Table 1
Monthly mean climate statistics for baseline (1961–1990) and deviations from baseline (future–baseline).

Month	Baseline climate			Deviations from baseline		
	T_{max} (°C)	T_{min} (°C)	Monthly precipitation (mm)	T_{max} (Δ°C)	T_{min} (Δ°C)	Monthly precipitation (% change)
1	0.9	−7.9	11.5	3.4	3.1	−14.6
2	3.9	−5.0	31.1	3.2	3.3	−0.8
3	9.5	0.5	60.0	2.9	2.7	2.8
4	15.4	6.2	92.1	2.3	2.4	8.2
5	21.3	12.0	109.9	3.2	2.8	10.9
6	26.9	17.5	105.2	3.3	3.2	8.2
7	29.5	20.6	103.6	3.2	3.1	7.9
8	28.3	19.5	78.3	4.5	4.0	2.9
9	23.2	14.1	49.1	3.4	4.1	42.1
10	15.8	6.7	31.1	2.9	3.4	30.3
11	8.5	−0.6	13.2	2.6	3.1	32.1
12	2.6	−6.3	5.5	3.5	3.5	35.5
Annual mean	15.5	6.4	690.5[a]	3.2	3.2	10.8

[a] Annual total.

Table 2
Sequence of field operations for each crop used in EPIC simulations. Numbers in parentheses denote quantity of fertilizer applied, kg ha^{-1}.

	Canola	Corn	Potato	Rice	Winter wheat
Up to planting	Field cultivate Spike harrow Fertilize N (100), P (40), K (40) Direct plant	Tan disk Tan disk Field cultivate Fertilize N (200) Row plant	Tan disk Point chisel Spike harrow Fertilize N (90), P (210) Row plant	Tan disk Field cultivate Tan disk Field cultivate Paddy bed Fertilize N (120) Plant DR	Moldboard plow Tan disk Field cultivate Fertilize N (150), P (55) Plant DR
Post-planting	Harvest	Row cultivate Row cultivate Harvest	Row cultivate Row cultivate Harvest	Irrigate (auto) Fertilize N (mid-season; 80) Harvest	Harvest
Post-harvest	Kill Tan disk Field cultivate	Kill Tan disk Point chisel	Potato truck Kill Moldboard plow	Kill Tan disk	Kill Moldboard plow

crop-sown areas from the Research Center for Eco-Environmental Sciences, Chinese Academy of Sciences, Beijing, and a Landsat thematic-mapper-derived land-cover map for all of mainland China (see Frolking et al., 2002).

2.5. Management

Table 2 lists the sequence of field operations employed for each crop in the EPIC model simulations. The timing of the operations follows a heat-unit-based schedule rather than rigid dates. The schedule anchors on the heat unit planting date (e.g. 15% of the fraction of the annual growing season) and growing season length (e.g. 2300 accumulated heat units) calculated using the EPIC PHU utility, which accounts for the unique monthly average climate statistics (T_{max}, T_{min}, elevation) at each location. The remaining field operations are then assigned heat unit schedule values relative to the planting date value. This feature allows for implicit adaptation to interannual temperature fluctuations and thus more realistically represents a dynamic farmer's decision-making. Values were calculated at each gridpoint for both the baseline and future climates to create climate-appropriate schedules for each period.

Adjustments to the above process were made in two specific cases. First, PHU values were not available for canola so these were calibrated using a location (30°N, 112.5°E) with similar climate characteristics as an existing study for Atlanta, GA (Raymer et al., 1990). Heat unit scheduling was then made to vary spatially in a manner proportional to the spatial variance found in winter wheat for the study region. Second, winter wheat heat unit scheduling values had to be adjusted to achieve realistic maximum crop heights at the start of the vernalization period. PHU for winter wheat planting were thus adjusted according to the equations $p_f = -.28p_0 + 1.16$ and $p_f = -.2p_0 + 1.13$ for the baseline and future periods, respectively, where p_0 is the PHU value calculated by the program and p_f is the adjusted value used in this study.

Table 2 also lists the quantity and type of fertilizer applied for each crop. In all cases except rice, fertilizer is applied at planting. In the case of rice, a mid-season application of 80 kg N ha^{-1} was made. The model was calibrated to match simulated denitrification with *in situ* measurements (Aulakh et al., 2001; Barton et al., 1999) and simulated N losses due to runoff with *in situ* measurements (Tian et al., 2007).

Given that a significant area of concern regarding climate change is its impact on the hydrological cycle (and, in turn, crop production), irrigation was not performed, except in the case of rice. Irrigation for rice was applied automatically as needed by EPIC at a minimum interval of 7 days. All internal model variables and parameters were held constant across space and simulations. Wind and water erosion were simulated, but slope and slope length were kept small, resulting in minimal impact due to water erosion.

2.6. EPIC model

2.6.1. Description

The EPIC model, version 0509, is a single-farm biophysical process model that can simulate crop/biomass production, soil evolution, and their mutual interaction given detailed farm management practices and input climate data (Williams, 1995). The model uses the concept of radiation-use efficiency (RUE) to simulate crop growth by calculating the potential daily photosynthetic production of biomass. EPIC computes actual growth by reducing potential growth by the largest multiplicative stress factor of the following stresses: shortages of water, nitrogen, phosphorus, and potassium; temperature extremes; and inadequate soil aeration. Stockle et al. (1992a,b) adapted EPIC to simulate the CO_2-fertilization effect on RUE and evapotranspiration (ET) to account for increased photosynthesis in C_3 plants and reduced ET in both C_3 and C_4 plants due to reduced stomatal conductance under conditions of elevated CO_2 concentrations, thereby improving water use efficiency. The equations governing this effect were derived from experimental data by Kimball (1983), which determined a crop yield increase of 33% under 2× CO_2 conditions with a 99% confidence interval of 24–43%. EPIC also dynamically accounts for soil C interactions in response to land use change, soil management, and climate change, and long-term field experiments have verified reasonable precision in representing these interactions in the US and Canada (Izaurralde et al., 2006).

2.6.2. Validation

The EPIC model has been validated at the global scale with favorable results (Tan and Shibasaki, 2003; Priya and Shibasaki, 2001). EPIC has also been validated extensively in many regions of the world under varying climates, soils, and management environments, including the US (e.g. Cavero et al., 1998; Chung et al., 1999; Izaurralde et al., 2003; Legler et al., 1999), Canada (e.g. Puurveen et al., 1997; Roloff et al., 1998), Italy (Rinaldi, 2001), Argentina (Bernardos et al., 2001), Great Britain (Boardman and Favis-Mortlock, 1993), India (Priya and Shibasaki, 2001), and China (Lu et al., 2003).

In the case of China, significant uncertainty exists in the accuracy of available agricultural data (Crook and Colby, 1996; Frolking et al., 1999; Gale et al., 2002; Verburg et al., 2000; Wang et al., 2002a,b) taken from a historical period during which rapid change in agricultural policy and reporting practice took place, resulting in exceptional increases in crop yields since 1960 (Tong et al., 2003; USDA, 2008). EPIC simulations by Sun

Table 3
Comparison of simulated yields with reported yield data.[a] Average EPIC simulated yields are 1961–1990 over the full study domain; maximum yields (in parentheses) are maximum 1961–1990 average yields at a single point in the domain.

Crop	Average EPIC simulated yield (max yield), Mg ha^{-1}	Reported yields, Mg ha^{-1}	Source
Canola	1.7 (2.4)	1.3	China 1990 (FAOSTAT, 2008)
		1.9–2.4	Southeast US with comparable climate (Raymer et al., 1990)
		1.7	Global average 2005 (Friedt et al., 2007)
Corn	4.5 (8.8)	4.5	China 1990 (USDA, 2008; FAOSTAT, 2008)
		4.1–5.9	Hebei, Shandong, Tianjin, and Beijing provinces (AED, 2009)
Potato	22.8 (34.4)	24	China 1991–1993 mean (Wang, 1997)
		10–28	Provinces in domain 1996 (Wang, 1997)
		17–23	Hebei, Shandong, Tianjin, and Beijing provinces (AED, 2009)
Rice	4.7 (6.8)	5.7	China 1990 (IRRI, 2008)
		4.0	China 1990 (USDA, 2008)
Winter wheat	2.5 (3.4)	3.2	China 1990 (USDA, 2008; FAOSTAT, 2008)
		3.7–5.4	Hebei, Shandong, Tianjin, and Beijing provinces (AED, 2009)

[a] Data from the end of the baseline period (1961–1990) better reflects the improved farm practices used as input in the EPIC model, and thus is used for validation in lieu of mean yields for the full period.

et al. (2001) replicated the historical trend of average provincial yields by increasing the planting density, fertilizer applications and irrigation each year. Thomson et al. (2006) compared EPIC simulations of winter wheat and maize yields to the Chinese Agricultural Economy Database, as well as to the Zhang et al. (1999) study of site-specific winter wheat experiment stations in the Huang-Hai Plain with favorable results. Overall, several other studies have recognized the Chinese data problem in model validation (Wang et al., 2002a,b; Lin, 1996; Matthews et al., 1997; Terjung et al., 1983). This is particularly true of rice, potato, and canola, for which few EPIC modeling studies have been performed in the region.

Thus, this study seeks to represent as best as possible the potential level of productivity based upon commonly accepted farm practices found in the literature and the general ranges of reported crop yields. From this baseline, estimates of relative productivity shifts due to climate change can help to identify vulnerable and emergent regions and crops. Given the aforementioned uncertainties, our focus is on the *relative* changes in productivity due to climate change.

Table 3 compares simulated yields with relevant available reported data. Average yields for all five crops compare favorably with reported data for the region, with the exception of slightly low simulated yields for winter wheat. This may be partly because the Huang-Hai Plain, the primary winter wheat production region, has low annual precipitation and therefore often requires irrigation (Smith and Klein, 2000) in the winter wheat–corn rotation system. We also compare the spatial distribution of crop yields with the 1990 UNH cropland dataset and find that key zones of crop cultivation match well with EPIC simulated regions of higher productivity.

2.6.3. Simulations performed in this study

Three separate full-domain simulations were performed in this study: baseline period 1961–1990, future period 2071–2100 under A2 scenario climate and CO_2 concentrations (hereafter 2071Y), and future period 2071–2100 under A2 scenario climate and baseline CO_2 concentrations (i.e. without enhanced CO_2-fertilization effect; hereafter 2071N). For the baseline and 2071N simulations, the CO_2 concentration in EPIC was set at 335 ppmv (1961–1990 average); for 2071Y, the CO_2 concentration was set at 740 ppmv (2071–2100 A2 average). For each simulation, two cold season crops (canola, winter wheat) and three warm season crops (corn, potato, rice) were grown throughout the domain. This approach allows for regional assessment of relative changes in crop productivity due to climate change, regardless of present-day ecological or economic viability in a given region.

2.7. Aggregation over the full domain

Each gridpoint from the 0.25×0.25 gridded RCM climate dataset is matched with the dominant soil profile at its location using GIS. Gridpoints are then matched to a cropland type using the UNH dataset of cropland area in each county. Finally, each gridpoint is given a heat-unit-based field operations schedule anchored on the calculated planting date and growing season length appropriate for the local climate. In this way the identical sequence of field operations is employed everywhere, but the timing of each operation during the year is an implicit function of accumulated heat units for the given year and location.

The EPIC model is run at each gridpoint for each of the dominant soils found at that location based on the following criteria: if the predominant soil proportion is at least 50%, it is the only soil used; if it is less than 50%, then runs are performed using all soils with proportions of at least 20%. Soils characterized as "rocky" are unsuitable for agriculture and not used in the simulations. The final result is 1–3 EPIC runs, each with a different soil profile, for each gridpoint. Supplemental EPIC runs were performed for counties in the domain that do not contain a gridpoint, using as inputs the primary soil polygon in the county and the weather and management data of the nearest gridpoint.

Final EPIC output is then aggregated to the county level using a linear weighted average:

$$Y_i = \frac{A_i}{m} \sum_{j=1}^{m} \sum_{k=1}^{3} \left(\frac{p_{jk}}{\sum_{k=1}^{3} p_{jk}} \right) y_{ijk},$$

where Y_i is the total county production (Mg) of crop i, A_i is the cultivated area (ha) for crop i, m is the total number of gridpoints in the county, p_{jk} is the proportion of soil k at gridpoint j, and y_{ijk} is the yield (Mg ha^{-1}) for crop i at gridpoint j with soil profile k. The quantity in parentheses is used to scale up the individual proportions to sum to 100%. If the simulated yield for a particular run within a county is greater than 40% below the average yield for all runs in that county, then the run is discarded under the assumption that cropland would not be located where crops grow poorly relative to nearby locations. This approach is used for all county-level output variables reported here. For counties along the domain border, cultivated area data (A_i) is adjusted according to

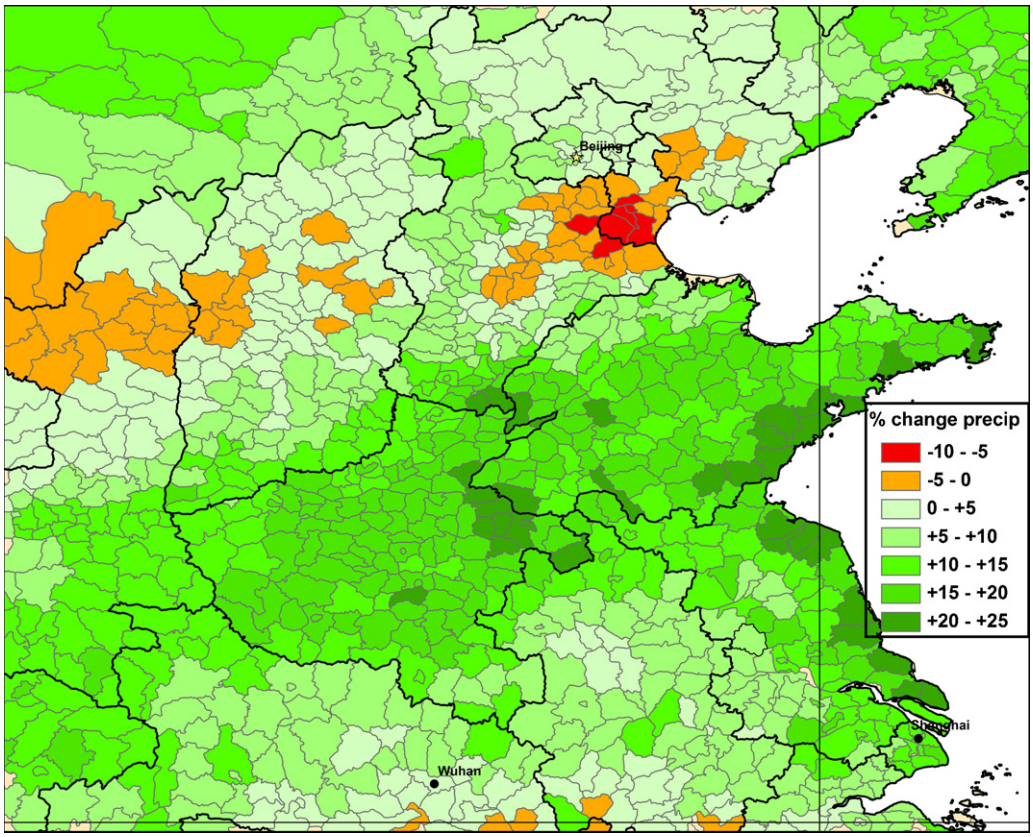

Fig. 3. Change (%) in mean annual precipitation between the future A2 scenario (2071–2100) and baseline (1961–1990).

approximate proportion of the total county area lying in the domain.

2.8. Statistical analysis of simulation results

Results were analyzed with SAS procedures (SAS Inst. Inc., Cary, NC). Mean separations were obtained with ANOVA using Fisher's least significant difference at the 0.1 level of probability. The REG procedure with the STEPWISE option (SLE = 0.1) was used to explain results variance by multiple linear regression.

3. Results

3.1. Climate change projections

3.1.1. Mean changes

For the full domain, the RCM for the future period (2071–2100) simulates an average annual precipitation increase of 75 mm (11%) relative to the baseline period (1961–1990), but with large spatial and temporal heterogeneity (Fig. 3). The most significant shift is a 20–25% increase in precipitation in a southwest–northeast oriented band north of the Yangtze River, covering much of the provinces of Shandong, Henan, and Jiangsu as well as southern Shaanxi and western Hubei in the southwestern corner of the domain (for causes see Gao et al., 2008). The lone region of decreased precipitation (0–10%) lies to the north in a parallel band that includes the provinces of Tianjin, central Hebei, and parts of Shanxi and northern Shaanxi. Precipitation is simulated to increase 3–42% primarily during the annual growing season (August–October), with January as the only month having a significant decrease in precipitation (15%).

Mean daily temperatures (as well as daily maximum and minimum) in the future period increase by an average of 3.2 °C, but with marked latitudinal variation. Temperatures increase by 2.5 °C in the South and by as much as 3.8 °C in the North. Temperature increases are distributed relatively uniformly throughout the year.

3.1.2. Changes in variability

Interannual variability of monthly mean temperatures remains constant in the future period. Interannual variability of monthly precipitation increases in the future period by 10% in January but decreases by 17% in November and 8% in December. For the remaining months variability change is small (0–2%).

3.2. Full-domain results

Differences between mean yields of each of the three scenarios are statistically significant based on ANOVA analysis. Simulated changes in aggregate potential productivity, defined as total production if the crop is grown on all 1990 cropland, for each crop in the future period under both current and future CO_2 concentrations are shown in Fig. 4. The most striking result is the significance of the enhanced CO_2-fertilization effect: under present CO_2 concentrations (2071N), future climate change has a negative impact on potential productivity of all five crops, ranging from a 2.5% decrease in canola to a 12% decrease in rice. However, under future elevated CO_2 concentrations (2071Y), future climate change has a significant positive impact on potential productivity of all five crops, ranging from a 6.5% increase in rice to a 25% increase in winter wheat. Similar results are reported at the national scale in the work of Lin et al. (2005) using alternative RCM output and the CERES crop simulation model. Recent findings from Free-Air CO_2 Enrichment (FACE) experiments have suggested that the effects of CO_2 enrichment in some crop models, including EPIC, may be overestimated (Long et al., 2006).

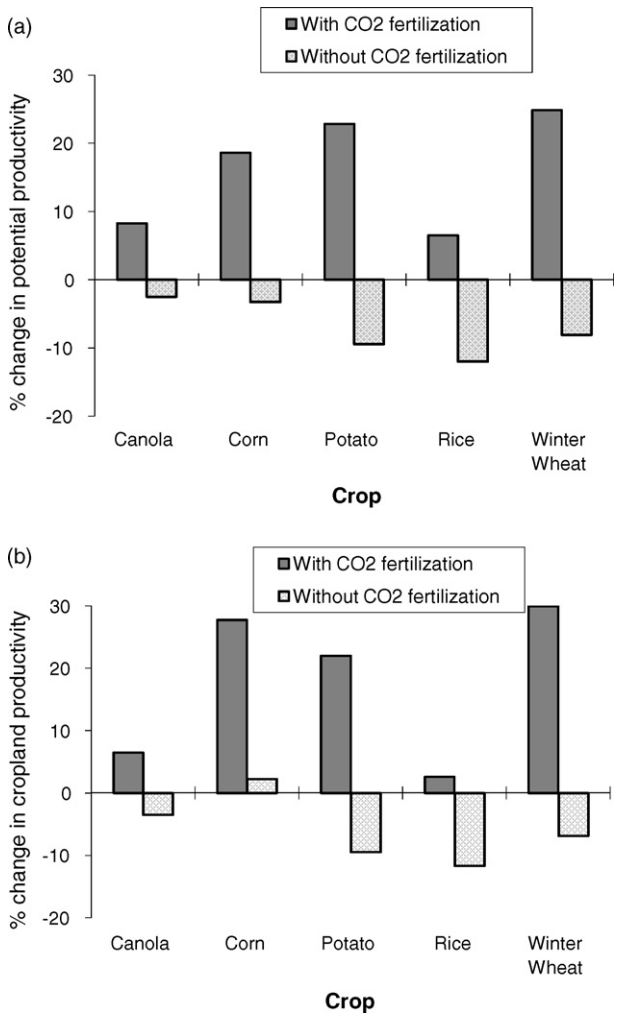

Fig. 4. Productivity shifts between the future A2 scenario (2071–2100) and baseline (1961–1990) for each crop under current (2071N) and future (2071Y) CO_2 concentrations. (a) Change (%) in aggregate production if the crop were grown everywhere in the domain. (b) Change (%) in aggregate production weighted by where the crop was actually grown in 1990.

A similar calculation is performed to assess changes in aggregate crop productivity based on 1990 county cropland area data specific to each crop (UNH). While significant change has occurred in China since 1990 the resulting estimated shifts in productivity are based on the actual spatial distribution of crop production in the region and therefore provide insight into how future production may change in the absence of adaptive changes. Overall, results under the crop-specific weighting scheme are similar to that of total potential productivity (Fig. 4), with the exception of corn, which shows productivity increases under *both* current and future CO_2 concentrations (2% and 28%, respectively).

Interannual yield variability, defined as the ratio of the standard deviation to the average yield at each location averaged across the full domain, decreases in 2071Y for corn (6%), potato (7%), and wheat (2%) while it increases for rice (4%) and remains constant for canola in the same time period (Table 4). Interannual yield variability is higher for all crops in the 2071N case, indicating that the CO_2-fertilization effect may reduce future yield variability.

Table 4
Normalized interannual yield variability (standard deviation as fraction of mean yield).

Normalized STD	1961	2071Y	2071N
Canola	0.27	0.27	0.29
Corn	0.59	0.53	0.64
Potato	0.35	0.28	0.30
Rice	0.16	0.20	0.22
Winter wheat	0.30	0.28	0.31

Table 5 lists the key variables whose relative changes explain simulated yield changes between 2071Y and baseline based upon regression analysis. Percent change in precipitation, wind speed, BD, LayerD, pH, sand content, and silt content and absolute change in temperature were tested. Overall, climate variables clearly play a more significant role than soil properties in explaining shifts in productivity for all crops, particularly in the cases of corn, canola, and winter wheat.

3.3. Regional variability

A primary purpose of this study was to identify regions of significant change in crop productivity, here defined as a greater than 10% increase (“emergent region”) or decrease (“vulnerable region”) in yields in the future period (2071–2100).

3.3.1. Canola

3.3.1.1. Vulnerable regions. With the exception of a single county in the domain, there are no significant regions of simulated declines in canola yield in the future period (Fig. 5(a)).

3.3.1.2. Emergent regions. The primary emergent region for canola is the North China Plain (NCP), particularly along the Huang He River, including southern Hebei, western Shandong, northern Henan, and southern Shanxi (Fig. 5(a)). Simulated yields increase 10–66%, with significant regions of 20–60% yield increases along the river. Regression analysis (Table 5) identifies temperature as the primary driver for change. A second emergent region is centered on southern and eastern Anhui province (10–15% yield increases). Regression analysis finds no significant correlations within Anhui but suggests that increased precipitation is a key driver in Jiangsu and Shanghai.

3.3.1.3. Current production regions. The primary canola producing region in 1990 is in the northwest (northwest Shanxi, northwest Hebei, Inner Mongolia provinces). Simulated yields in this region remain relatively constant.

3.3.2. Corn

3.3.2.1. Vulnerable regions. Two key vulnerable regions for corn production exist: along the southern edge of the domain (Hubei, Anhui) and in northern Shaanxi (Fig. 5(b)). In the former, EPIC simulates 10–20% losses in productivity. Regression analysis reveals that a key driver in this region is precipitation, which remains constant or declines under warmer temperatures and leads to increases in water stress of 1–9 days annually. In northern Shaanxi, EPIC simulates 20–40% yield decreases. This region is co-located with a pocket of decreased precipitation, resulting in increased water stress as the likely cause of decreased productivity.

3.3.2.2. Emergent regions. The key emergent corn production region exists through the center of the domain, including Shandong, Henan, northern Anhui, northern Jiangsu, southern Shanxi, southern Hebei, and central Shaanxi provinces. Simulated yields in this region increase 10–66% (Fig. 5(b)), with increases of 80–200% along the Henan–Shanxi and Henan–Hebei province borders. Regression results show a combination of temperature and precipitation as the primary driver of productivity change

Table 5
Key variables, listed in order of significance, for explaining variance in crop yield changes for each crop, derived from the SAS multiple linear regression of changes (%) in yield vs. changes in various climate and soil variables between 2071Y and baseline. R^2 values, given in parentheses, are cumulative with the addition of each variable to the regression model. Only variables that explain >5% variance (10% for initial variable) are included.

Province	Canola			Corn			Potato		
	1st	2nd	3rd	1st	2nd	3rd	1st	2nd	3rd
Inner Mongolia	BD (.25)			Wind (.34)	Prec (.42)		BD (.19)	Wind (.29)	
Shaanxi	Wind (.12)			Prec (.27)	BD (.4)		Silt (.01)		
Shanxi	Temp (.26)	Wind (.38)		Prec (.62)			Wind (.17)	BD (.23)	
Hebei	Temp (.48)			Prec (.45)	BD (.54)	Temp (.59)	BD (.23)	Wind (.3)	
Liaoning	NSS[a]			Wind (.11)	BD (.19)	Temp (.26)	Temp (.64)	Wind (.7)	
Henan	Temp (.29)			Temp (.62)			Temp (.47)		
Shandong	Temp (.39)	BD (.47)		BD (.09)			Temp (.54)	Sand (.63)	Wind (.68)
Hubei	Temp (.21)			Prec (.3)	BD (.35)		Temp (.17)	Sand (.24)	
Anhui	Wind (.01)			Temp (.51)	Wind (.61)	Prec (.76)	Temp (.32)	Wind (.45)	LayerD (.5)
Jiangsu	Prec (.24)	Wind (.32)		Prec (.46)	Temp (.71)		Temp (.2)		
Shanghai	Prec (.46)	BD (.63)	Temp (.73)	Wind (.76)			Prec (.29)		

Province	Winter wheat			Rice		
	1st	2nd	3rd	1st	2nd	3rd
Inner Mongolia	Wind (.27)	Prec (.39)		BD (.65)	Wind (.8)	
Shaanxi	Prec (.61)			Prec (.36)	BD (.62)	LayerD (.69)
Shanxi	Temp (.58)			Temp (.78)	Wind (.88)	
Hebei	Wind (.46)	Temp (.65)	Prec (.7)	Wind (.52)	Temp (.79)	Prec (.87)
Liaoning	Temp (.1)	Wind (.29)		Temp (.6)	BD (.67)	
Henan	Temp (.25)	BD (.3)	Prec (.35)	BD (.15)	Prec (.34)	
Shandong	Temp (.16)			NSS[a]		
Hubei	Wind (.08)			NSS[a]		
Anhui	Temp (.32)	Wind (.43)		Temp (.39)	BD (.47)	
Jiangsu	Temp (.71)			Temp (.36)		
Shanghai	Temp (.62)	Prec (.84)		None		

[a] Not statistically significant.

(Table 5). This suggests that the emergence of this region can be viewed as a northward (and westward, near the coast) shift in the high-productivity "corn belt" currently located in the southern tier of the domain. This shift is a result of warmer temperatures expanding northward and overlapping with the area of increased precipitation stretching southwestward from the Yellow Sea. A second emergent region lies along the northern border of the domain (Inner Mongolia, northern Shanxi, northern Hebei, western

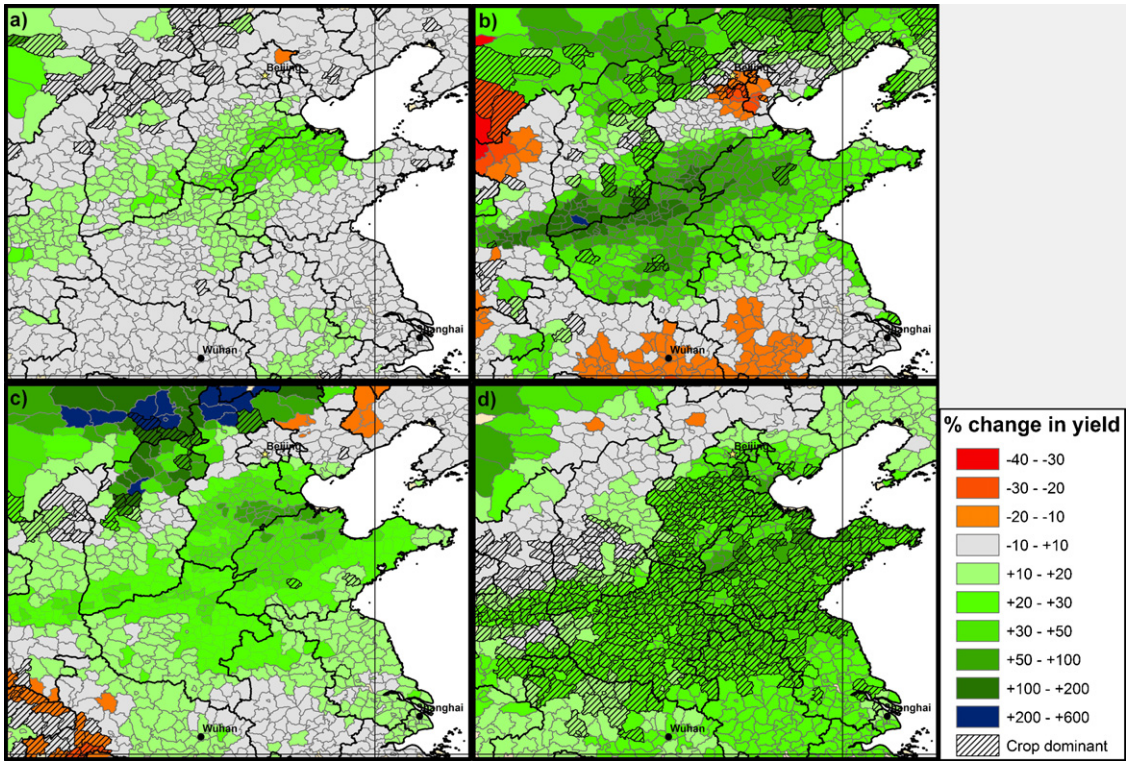

Fig. 5. Change (%) in yield between the future A2 scenario (2071Y) and baseline for (a) canola; (b) corn; (c) potato; (d) winter wheat. Hatching indicates the given crop is dominant in the county based on 1990 cropland area data. Note: economic feasibility is not incorporated into the results presented here (see Section 4).

Liaoning), where yields increase 20–80% from relatively low baseline yields of 1–3 Mg ha^{-1}. Regression results indicate changes in precipitation as the key driver to the northwest and both soil and climate drivers to the northeast.

3.3.2.3. Current production regions. The primary regions of corn production in 1990 are in the North China Plain and in the northeast corner of the domain (Liaoning province). In both cases, EPIC simulates yield increases of 10–40% in the future period. Lesser but nonetheless positive yield increases also occur in the absence of enhanced CO_2 fertilization.

3.3.3. Potato

3.3.3.1. Vulnerable regions. Two vulnerable potato producing regions are the southwest (western Hubei, eastern Sichuan, southern Shaanxi provinces) and the northeast (western Liaoning). In the southwest, EPIC simulates 10–20% decreases in crop productivity in several counties (Fig. 5(c)). Regression results are hampered by small sample size, but in Hubei there is a strong anti-correlation between temperature and yield, suggesting that temperatures are warming beyond optimal temperature for potato growth and reducing productivity. There is also a small pocket of declining yields in the northeast (western Liaoning), where EPIC simulates 10–15% yield declines for similar reasons.

3.3.3.2. Emergent regions. The first emergent potato growing region is the far northwest and north central portion of the domain (Inner Mongolia, northern Hebei, northern Shanxi). EPIC simulated yields increase 30–600% (Fig. 5(c)) from low baseline yields of ~1–2 Mg ha^{-1}. Regression results indicate that the primary driver is related to wind and soil properties, as this is a region where wind erosion is significant in the baseline period but decreases under the climate change projections used here. Productivity in this region increases dramatically (up to 350%) in the 2071N simulation case as well. The second emergent region is the North China Plain (Beijing, Tianjin, Henan, Shandong provinces), where yields increase 10–80% due primarily to warmer temperatures. Furthermore, this region of high yields, relative to surrounding areas, largely disappears in the 2071N simulation. This indicates (as with canola) the importance of elevated CO_2 concentrations, which enhances water use efficiency, in regions where drought is commonplace. In the 2071Y case water stress decreases 3–6 days annually, whereas in the 2071N case water stress remains constant.

3.3.3.3. Current production regions. The primary region of potato production in 1990 is located in the far southwestern portion of the domain, where EPIC simulates significant future yield losses. Potato is also the dominant crop in several counties in the northwest, where yields are expected to increase dramatically. Finally, significant production occurs in northwestern Anhui, where 10–25% increases in yields are simulated in the future period.

3.3.4. Winter wheat

3.3.4.1. Vulnerable regions. No significant vulnerable region is identified from the EPIC simulations, as only two counties have simulated yield decreases greater than 10% (Fig. 5(d)).

3.3.4.2. Emergent regions. Much of the North China Plain (northwestern Shandong, southern Hebei, northern Henan) has simulated winter wheat productivity increases of 30–70% (Fig. 5(d)). This area is part of a larger region where yield increases of at least 10% are simulated. The largest productivity increases are found along the coast of the Yellow Sea, although winter wheat productivity looks to be greatly enhanced throughout the domain under simulated future climate conditions. Regression analysis suggests warmer temperatures are a key contributor to increased productivity in this region.

3.3.4.3. Current production regions. The principal winter wheat production region in 1990 lies just to the north of the southern rice belt (northern Hubei, Henan, northern Anhui, northern Jiangsu, and Shandong provinces). EPIC simulates 20–40% yield increases in the future period.

3.3.5. Rice

3.3.5.1. Vulnerable regions. The lone region of significant decreases in simulated yields exists in Henan province, where EPIC simulates crop productivity losses of 10–15% in the future period (Fig. 6(a)). Regression results do not indicate one primary factor; however, this region is co-located with a region of substantial increases in temperature stress (6–13 days annually). In the South, the dominant stress on the crop shifts from temperature to nitrogen, suggesting that productivity gains may be possible via increased fertilizer input.

3.3.5.2. Emergent regions. The primary emergent region for rice production is the northern 1/5 of the domain and the northwest (northern Shaanxi, Shanxi, Inner Mongolia, northern Hebei,

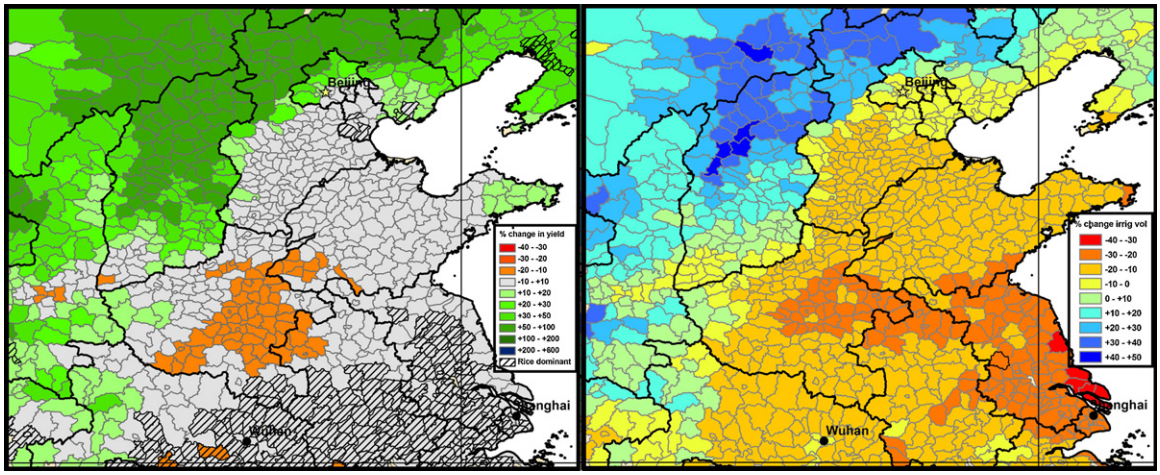

Fig. 6. (a) As in Fig. 5(a)–(d) but for rice. (b) Change (%) in irrigation volume for simulated rice between 2071Y and baseline. Note: irrigation values should be taken into account when evaluating rice yield shifts, as the capacity to achieve simulated yields is dependent upon local water resource availability and economic conditions, which are highly uncertain and not assessed in this study.

Liaoning provinces), although the "emergence" of this region is dependent upon substantial irrigation inputs in a region that already faces water deficits, particularly in the northwest where EPIC simulates a co-located 15–50% increase in irrigation needs. EPIC simulates 20–97% increases in crop productivity in the northeast due primarily to longer growing seasons (Fig. 6(a)); irrigation remains relatively constant. Thus, the northeast may be the only emergent region where simulated yield increases are economically feasible, although further analysis is needed.

3.3.5.3. Current production regions. The chief 1990 rice production region in the domain lies south and east of a line stretching from south-central Hubei to the northeast coast of Jiangsu (southeastern Hubei, southern Anhui, Jiangsu, Shanghai, Zhejiang provinces). EPIC does not simulate any significant changes in productivity in this region. Furthermore, EPIC simulates a 5–37% decrease in irrigation needs and 10–40 day decline in annual temperature stress days, particularly towards the coast. This finding, coupled with the aforementioned emergence of nitrogen deficiency as the dominant stress in the future period, suggests that increased farm inputs may lead to greater productivity gains (or offset losses) than simulated in this study.

The secondary rice production region lies in the northeast (northeast Hebei, Liaoning provinces). EPIC simulates yield increases of 20–97%, with higher values towards the northeast corner.

4. Discussion

Across all crops simulated in this work, the southwest appears to suffer the most under climate change by 2100, as yields decline for potato (the dominant crop), canola and corn, and increase only marginally for winter wheat and rice. The south and southeast appear likely to remain predominantly rice growing regions despite simulated yield declines. In the North China Plain, simulations suggest that the predominant corn-winter wheat crop rotation will benefit significantly from warmer temperatures and increased precipitation. To the northwest, simulated increased precipitation in a region that is currently very dry may help to support much improved crop productivity, in particular corn and potato. Finally, to the northeast, simulations suggest that rice and corn will emerge as the most productive crops under future climate conditions.

Overall results agree reasonably well with other similar studies. Simulated increases in rain-fed corn production largely agree with that found by Xiong et al. (2007) in the Huang-Hai plain region, including the vulnerable region near the Yellow Sea coast to the east of Beijing. Productivity shifts for rice (+4.3%), winter wheat (+23.6%), and corn (+20.3%) found by Lin et al. (2005) at the national scale correspond closely with the results presented here, including the significant simulated positive effect of CO_2 enrichment in all cases. Rice productivity increases in this work are larger than that found by Tao et al. (2008) under a 3-degree increase in global mean temperature.

We note that significant limitations exist in the capacity to evaluate both current and future agricultural productivity in China. This includes uncertainties in and limited access to Chinese crop production, farm management, and terrain data at the local level; climate model uncertainty, particular regarding precipitation patterns; knowledge of future adaptation via shifts to warmer-climate varieties and other farm practices; and representation of changes in soils between the baseline and future periods. Thus, we focus solely on relative rather than absolute shifts in productivity under basic management practices to tease out changes in crop yields due primarily to changes in climate. Furthermore, given the economic and political complexity underlying agricultural decision-making that lies beyond the scope of this study, the authors choose not to exclude any data based on threshold values of crop yield (e.g. in the case of a county with low simulated baseline yields but large relative yield changes) or irrigation (e.g. in the case of irrigation needs that exceed local water resource availability) as a metric of economic feasibility. Such thresholds are highly uncertain for long time horizons and are relatively arbitrary without an in-depth economic analysis and forecast that is reserved for future work.

5. Conclusions

The results of this study belie the significant vulnerability of crop productivity and food security to changes in climate. By the end of the 21st century under A2 scenario climate conditions, EPIC simulations indicate that crop productivity in eastern China is expected to increase, although with substantial spatial variation linked primarily to regional precipitation patterns. In key present-day crop production zones, corn and winter wheat yields increase substantially, potato yields decline substantially, canola yields remain relatively constant, and rice yields may decrease inland and increase towards the coast, although increased nitrogen input may boost rice yields throughout. Absent CO_2 enrichment, however, climate change negatively impacts aggregate crop productivity in the domain except in the case of corn.

Much more work is needed to fully assess the potential impacts of climate change on agriculture in our domain of interest and, more importantly, the proper adaptive responses by farmers and policy-makers. Using input data from multiple climate models and multiple scenarios can provide better insight into the potential range of impacts and associated probabilities. Furthermore, coupling with economic models is needed in order to determine optimal strategies for crop production based on the shifting costs and benefits of growing particular crops under future climate conditions.

Acknowledgements

This work was supported by the US Department of Energy–China Meteorological Administration Bilateral Agreement on the Study of Regional Climate and the US DOE Office of Biological and Environmental Research under contract DE-AC06-76RLO 1830. We gratefully acknowledge the assistance of Changsheng Li and Steve Frolking of the University of New Hampshire, as well as Shaoqiang Wang, Jay Gregg, Jimmy Williams, and Todd Campbell.

References

AED, 2009. Agricultural Economy Database prepared by the Institute of Geographical Sciences and Natural Resources Research at the Chinese Academy of Sciences (http://www.naturalresources.csdb.cn/ny/cdroom/tx2new.asp).

Aulakh, M.S., Khera, T.S., Doran, J.W., Bronson, K.F., 2001. Denitrification, N_2O and CO_2 fluxes in rice–wheat cropping system as affected by crop residues, fertilizer N and legume green manure. Biol. Fertil. Soils 34, 375–389.

Barton, L., McLay, C.D.A., Schipper, L.A., Smith, C.T., 1999. Annual denitrification rates in agricultural and forest soils: a review. Aust. J. Soil Res. 37, 1073–1093.

Batjes, N.H., 2006. ISRIC-WISE derived soil properties on a 5 by 5 arc-minutes global grid. Report 2006/02 (available through: http://www.isric.org), ISRIC-World Soil Information, Wageningen (with data set).

Bernardos, J.N., Viglizzo, E.F., Jouvet, V., Lértora, F.A., Pordomingo, A.J., Cid, F.D., 2001. The use of EPIC model to study the agroecological change during 93 years of farming transformation in the Argentine pampas. Agric. Syst. 69 (3), 215–234.

Boardman, J., Favis-Mortlock, D.T., 1993. Climate change and soil erosion in Britain. Geograph. J. 159 (2), 179–183.

Canpeng, L., Wenhui, C., Jianbin X., 1999. The state of the land, water and plant nutrient resources in China (http://www.fjtu.edu.cn).

Cavero, J., Plant, R.E., Shennan, C., Williams, J.R., Kiniry, J.R., Benson, V.W., 1998. Application of EPIC model to nitrogen cycling in irrigated processing tomatoes under different management systems. Agric. Syst. 56, 391–414.

Cheng, C. (Ed.), 1993. Climate and Agriculture in China. China Meteorological Press, Beijing, 519 pp.

Chung, S.W., Gassman, P.W., Kramer, L.A., Williams, J.R., Gu, R., 1999. Validation of EPIC for two watersheds in southwest Iowa. J. Environ. Qual. 28, 971–979.
Crook, F.W., Colby, W.H., 1996. The future of China's grain market. In: Agricultural Information Bulleting Number 730, US Department of Agriculture, Economic Research Service, Washington, DC, 24 pp.
Downing, T.E. (Ed.), 1996. Climate Change and World Food Security NATO ASI Series I: Global Environmental Change 37. Spring, Berlin, 662 pp.
FAOSTAT, 2008. United Nations' Food and Agricultural Organization (FAO), Statistical Database on Production, ProdSTAT, FAOSTAT (http://faostat.fao.org/site/567/default.aspx).
Friedt, W., Snowdon, R., Ordon, F., Ahlemeyer, J., 2007. Plant breeding: assessment of genetic diversity in crop plants and its exploitation in breeding. Prog. Bot. 68, 151–178.
Frolking, S., Xiao, X., Zhuang, Y., Salas, W., Li, C., 1999. Agricultural land use in China: a comparison of area estimates from ground-based census and satellite-borne remote sensing. Glob. Ecol. Biogeogr. 8, 407–416.
Frolking, S., Qiu, J., Boles, S., Xiao, X., Liu, J., Zhuang, Y., Li, C., Qin, X., 2002. Combining remote sensing and ground census data to develop new maps of the distribution of rice agriculture in China. Glob. Biogeochem. Cycles 16 (4), 1091.
Gale, F., Tuan, F., Lohmar, B., Hsu, H., Gilmour, B., 2002. China's food and agriculture: issues for the 21st century. USDA Economic Research Service Agricultural Information Bulletin no. AIB775. Washington, DC, 64 pp.
Gao, X., Shi, Y., Song, R., Giorgi, F., Wang, Y., Zhang, D., 2008. Reduction of future monsoon precipitation over China: comparison between a high resolution RCM simulation and the driving GCM. Meteorol. Atmos. Phys. 99 , doi:10.1007/s00703-008-0296-5.
IPCC, 2007. In: Solomon, S., Qin, D., Manning, M., Chen, Z., Marquis, M., Averyt, K.B., Tignor, M., Miller, H.L. (Eds.), Climate Change 2007: The Physical Science Basis. Contribution of I to the Fourth Assessment Report of the Intergovernmental Panel on Climate Change. Cambridge University Press, Cambridge, United Kingdom and New York, NY, USA, p. 996.
IRRI, 2008. Rough rice yield, by country and geographical region-FAO (http://www.irri.org/science/ricestat/data/may2008/WRS2008-Table03.pdf).
Izaurralde, R.C., Rosenberg, N.J., Brown, R.A., Thomson, A.M., 2003. Integrated assessment of Hadley Center (HadCM2) climate-change impacts on agricultural productivity and irrigation water supply in the conterminous United States. Part II. Regional agricultural production in 2030 and 2095. Agric. For. Meteorol. 117, 97–122.
Izaurralde, R.C., Williams, J.R., McGill, W.B., Rosenberg, N.J., Quiroga Jakas, M.C., 2006. Simulating soil C dynamics with EPIC: model description and testing against long-term data. Ecol. Model. 192, 362–384.
Kimball, B.A., 1983. Carbon dioxide and agricultural yield: an assemblage of analysis of 430 prior observations. Agron. J. 75, 779–788.
Legler, D.M., Bryant, K.J., O'Brien, J.J., 1999. Impact of ENSO-related climate anomalies on crop yields in the US. Clim. Change 42, 351–375.
Li, C., Zhuang, Y., Frolking, S., Galloway, J., Harriss, R., Moore III, B., Schimel, D., Wang, X., 2003. Modeling soil organic carbon change in croplands of China. Ecol. Appl. 13 (2), 327–336.
Lin, E., 1996. Agricultural vulnerability and adaptation to global warming in China. Water Air Soil Pollut. 92, 63–73.
Lin, E., Xiong, W., Ju, H., Xu, Y., Li, Y., Bai, L., Liyong, X., 2005. Climate change impacts on crop yield and quality with CO_2 fertilization in China. Philos. Trans. R. Soc. B 360, 2149–2154.
Long, S.P., Ainsworth, E.A., Leakey, A.D., Nösberger, J., Ort, D.R., 2006. Food for thought: lower-than-expected crop yield stimulation with rising CO_2 concentrations. Science 312 (5782), 1918–1921.
Lu, C.H., Ittersum, M.K., van, Rabbinge, R., 2003. Quantitative assessment of resource-use efficient cropping systems: a case study for Ansai in the Loess Plateau of China. Eur. J. Agron. 19, 311–326.
Matthews, R.B., Kropff, M.J., Horie, T., Bachelet, D., 1997. Simulating the impact of climate change on rice production in Asia and evaluating options for adaptation. Agric. Syst. 54 (3), 399–425.
Nakicenovic, N., Alcamo, J., Davis, G., et al., 2000. Special report on emissions scenarios: a special report of Working Group III to the fourth assessment report of the intergovernmental panel on climate change. Cambridge University Press, Cambridge, UK, 600 pp.
Priya, S., Shibasaki, R., 2001. National spatial crop yield simulation using GIS-based crop production model. Ecol. Model. 135, 113–129.
Puurveen, H.P., Izaurralde, R.C., Chanasyk, D.S., Williams, J.R., Grant, R.F., 1997. Evaluation of EPIC's snowmelt and water erosion submodels using data from the Peace River region of Alberta. Can. J. Soil Sci. 77, 41–50.
Qian, W., Zhu, Y., 2001. Climate change in China from 1880 to 1998 and its impact on the environmental condition. Clim. Change 50, 419–444.
Raymer, P.L., Bullock, D.G., Thomas, D.L., 1990. Potential of winter and spring rapeseed cultivars for oilseed production in the southeastern United States. In: Janick, J., Simon, J.E. (Eds.), Advances in New Crops. Timber Press, Portland, OR, pp. 223–225.
Rinaldi, M., 2001. Application of EPIC model for irrigation scheduling of sunflower in Southern Italy. Agric. Water Manage. 49, 185–196.
Roloff, G., de Jong, R., Zentner, R.P., Campbell, C.A., Benson, V.W., 1998. Estimating spring wheat yield variability with EPIC. Can. J. Soil Sci. 78, 541–549.
Smith, E., Klein, K.K., 2000. Development and adoption of dryland cropping technologies in Hebei province of northern China. Can. J. Agric. Econ. 48, 573–583.
Soil Map of the People's Republic of China, 1990. Revised version based on the FAO/UNESCO soil map of the world (http://eusoils.jrc.it/esdb_archive/EuDASM/asia/lists/ccn.htm).
Stockle, C.O., Dyke, P.T., Williams, J.R., Allen, C.A., Rosenberg, N.J., 1992a. A method for estimating direct and climatic effects of rising atmospheric carbon dioxide on growth and yield of crops. Part II—Sensitivity analysis at three sites in the Midwestern USA. Agric. Syst. 38, 239–256.
Stockle, C.O., Williams, J.R., Rosenberg, N.J., Allen, C.A., 1992b. A method for estimating direct and climatic effects of rising atmospheric carbon dioxide on growth and yield of crops. Part I—Modification of the EPIC model for climate change analysis. Agric. Syst. 38, 225–228.
Sun, L., Rosenberg, N.J., Izaurralde, R.C., 2001. Assessment of climate change impacts on agriculture in the northern part of the North China Plain. PNNL Technical Report 13546. Pacific Northwest National Laboratory, Richland, WA, 35 pp.
Tan, G.X., Shibasaki, R., 2003. Global estimation of crop productivity and the impacts of global warming by GIS and EPIC integration. Ecol. Model. 168, 357–370.
Tao, F., Yokozawa, M., Hayashi, Y., Lin, E., 2003. Future climate change, the agricultural water cycle, and agricultural production in China. Agric. Ecosyst. Environ. 95, 203–215.
Tao, F., Hayashi, Y., Zhang, Z., Sakamoto, T., Yokozawa, M., 2008. Global warming, rice production, and water use in China: developing a probabilistic assessment. Agric. For. Meteorol. 148 (1), 94–110.
Tao, S.Y., Chen, L.X., 1987. In: Chang, C.P., Krishnamurti, T.N. (Eds.), A Review of Recent Research on the East Asian Summer Monsoon in China. Monsoon Meteorology. Oxford University Press, pp. 60–92.
Terjung, W.H., Ji, H.-Y., Hayes, J.T., O'Rourke, P.A., Todhunter, P.E., 1983. Actual and potential yield for rainfed and irrigated maize in China. Int. J. Biometeorol. 28 (2), 115–135.
Thomson, A.M., Izaurralde, R.C., Rosenberg, N.J., He, X., 2006. Climate change impacts on agriculture and soil carbon sequestration potential in the Huang-Hai Plain of China. Agric. Ecosyst. Environ. 114 (2–4), 195–209.
Tian, Y., Yin, B., Yang, L., Yin, S., Zhu, Z., 2007. Nitrogen runoff and leaching losses during rice-wheat rotations in Taihu Lake Region, China. Pedosphere 17 (4), 445–456.
Tian, Z., 2006. A study on the impact of climate change on the potential productivity in Huang-Huai-Hai plain in China. Institute of Geography Science and Nature Resource, Chinese Academy of Science, 149 pp. (http://www.aslo.org/phd/disccrs/200607-6.html).
Tong, C., Hall, C.A.S., Wang, H., 2003. Land use change in rice, wheat and maize production in China (1961–1998). Agric. Ecosyst. Environ. 95, 523–536.
United States Department of Energy, 2004. World energy and economic outlook. In: Energy Information Administration, US DOE, Washington, DC.
USDA, 2008. Crop production historical track records. United States Department of Agriculture Foreign Agricultural Service (http://usda.mannlib.cornell.edu/usda/current/htrcp/htrcp-04-30-2008.pdf).
Verburg, P.H., Chen, Y., Veldkamp, T.A., 2000. Spatial explorations of land use change and grain production in China. Agric. Ecosyst. Environ. 82, 333–354.
Wang, E., Harman, W.L., Williams, J.R., Xu, C., 2002a. Simulated effects of crop rotations and residue management on wind erosion in Wuchan, West-Central Inner Mongolia, China. J. Environ. Qual. 31, 1240–1247.
Wang, S., Zhou, C., Liu, J., Tian, H., Li, K., Yang, X., 2002b. Carbon storage in northeast China as estimated from vegetation and soil inventories. Environ. Pollut. 116 (Suppl.), S157–S165.
Wang, Y., 1997. Overview of Potato Production in China. International Potato Center (http://www.eseap.cipotato.org/MF-ESEAP/FI-Library/Pto-China.pdf).
Watson, R., Zinyowera, M., Moss, R. (Eds.), 1996. Climate change 1995—impacts, adaptation and mitigation of climate change. Contribution of Working Group II to the Second Assessment Report of the IPCC. Cambridge University Press, Cambridge.
Williams, J.R., 1995. The EPIC model. In: Singh, V.P. (Ed.), Computer Models in Watershed Hydrology. Water Resources Publication, Highlands Ranch, CO, pp. 909–1000.
World Bank, 2002. China Country Water Resources Assistance Strategy. The World Bank East Asia and Pacific region (http://siteresources.worldbank.org/INTWRD/Resources/ChinaCountryWaterResourcesAssistanceStrategy.pdf).
Xiong, W., Matthews, R., Holman, I., Lin, E., Xu, Y., 2007. Modelling China's potential maize production at regional scale under climate change. Climatic Change 85 (3–4), 433–451.
Zhang, H., Wang, X., You, M., Liu, C., 1999. Water–yield relations and water-use efficiency of winter wheat in the North China Plain. Irrig. Sci. 19, 37–45.